ISBN: 978-3-95450-194-6 doi:10.18429/JACoW-LINAC2018-TUPO020

MICROPHONICS INVESTIGATION OF ARIEL e-LINAC CRYOMODULES

Yanyun Ma†, K. Fong, M. Keikha, J. Keir, D. Kishi, S.R. Koscielniak, D. Lang, R.E. Laxdal, R. Nagimov, Z.Y. Yao, Q.W. Zheng, V. Zvyagintsev
TRIUMF, 4004 Wesbrook Mall, Vancouver, BC, Canada
Lutz Lilje, DESY, Notkestrasse 85, D-22607 Hamburg, Germany

Abstract

Now the stage of the 30 MeV portion of ARIEL (The Advanced Rare Isotope Laboratory) e-Linac is under commissioning which includes an injector cryomodule (ICM) and the 1st accelerator cryomodule (ACM1) with two cavities configuration. In this paper, the progress of the microphonics investigation and suppression of ICM and ACM1 is presented.

INTRODUCTION

ARIEL e-Linac is a continuous-wave (CW) electron linear accelerator utilizing superconducting bulk niobium technology at 1.3 GHz. The accelerator is divided into three cryomodules [1, 2]: a single cavity injector cryomodule (ICM) and two accelerating cryomodules (ACM) with two cavities each. The 'Demonstrator' phase of ARIEL was installed for initial technical and beam tests [3]. Then ACM1 cryomodule, high-power RF distribution system and LLRF system were updated for 2 cavities [4]. During commissioning, acoustic noise from the environment vibration generated by cooling water pumps, cryogenic system and vacuum system affect the ACM1 RF performance and final beam energy stability.

PONDERMOTIVE EFFECT

Both ICM and ACM1 are working in phase-locked loop (PLL) self-excited loop (SEL) in CW mode. Unlike the ICM with one cavity and one SEL loop, the two ACM1 cavities are driven by a single klystron with vector-sum control of the two cavity SEL PLL. As such there is no gradient regulation for each individual cavity in the ACM1 [5]. Individual tuner loops are established to maintain the cavity frequency with respect to the established reference phase. Microphonics can excite mechanical resonances in one cavity, perturbing the RF resonant frequency, which can couple to the other cavity via vector-sum regulation. The modulations of the RF field between the two cavities can drive a ponderomotive instability through Lorentz force detuning. The threshold for excitation of this instability is impacted both by ambient microphonic noise that can seed the instability and the precise settings of the two cavity phase loops. The coupled oscillation can deteriorate the e-Linac final energy stability outside specification and needs to be controlled.

During the commissioning, the ACM1 cavities gradients were limited by the ponderomotive effect when the summed voltage was higher than 17 MV. The ACM1 cavities pickup signals showed oscillation in counterphase (Fig. 1) while under vector-sum regulations impacting the energy stability and ultimately the loop stability.

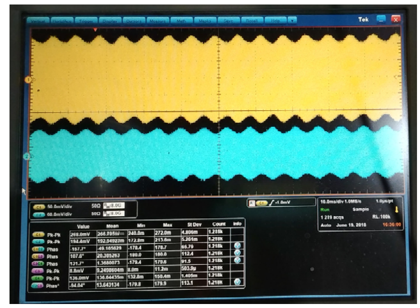

Figure 1: The ponderomotive oscillation of ACM1 pickup signals. The yellow waveform is 1st cavity pickup signal and the green waveform is 2nd cavity pickup signal.

NOISE OF PICKUP SIGNALS

To identify the noise peak for each cavity, the ACM1 was switched from vector-sum mode to single cavity mode and the pickup signals were analysed by phase noise analyser (R&S®FSWP26). Figure 2 shows that there is a noise hump from 10Hz to 400Hz in each pickup signal and indicates the noise sources are universal for all three cavities.

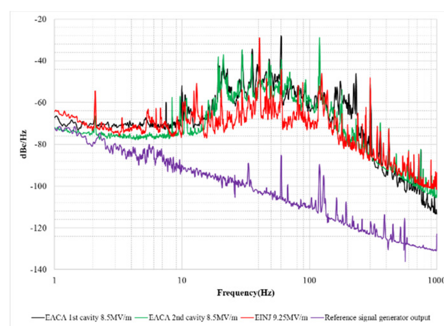

Figure 2: pickup signals noise analyses. During the test the ACM1 was setup in single cavity mode with closed amplitude and phase loop with low proportional gain; the ICM was under operational mode.

The coupling between microphonic noise disturbances and Lorentz force has been measured on ACM1 cavities. Amplitude modulations of various frequencies were added onto the amplitude loop driver while keep the amplitude loop and phase loop closed and fixed tuners position. Both cavities were measured at the similar e-field level. The parameters of the first 5 strongest microphonic disturbances coupling to Lorentz force are listed in Table.1.

† mayanyun@triumf.ca

ISBN: 978-3-95450-194-6 doi:10.18429/JACoW-LINAC2018-TUPO020

Table 1. Noise Peaks of ICM and ACM1 Pickup Signals

	Frequency (Hz)	Power (dBc/Hz)	Q	K (Hz/(MV/m)^2)
ICM	40.70	-31.60	68.7	
	124.66	-43.57	53.7	
	60.01	-48.38	85.7	
	300.09	-49.76	241.6	
	46.08	-51.26	36.5	
ACM1 1st cavity	59.96	-30.20	96.7	0.2294
	119.96	-36.33	66.6	0.1601
	35.57	-36.66	57.4	0.2359
	48.30	-42.19	60.4	0.3694
	29.66	-42.28	84.7	0.1575
	232.18	-43.11	114.9	0.0727
ACM1 2nd cavity	120.04	-28.87	135.3	0.1386
	35.27	-42.08	93.7	0.1664
	60.02	-44.77	199.9	0.0937
	29.60	-45.15	59.2	0.1597
	47.90	-45.77	159.7	0.0712

MECHANICAL VIBRATION SOURCE

The external vibrations couple to the mechanical system constituted of the cavity and auxiliary components and excite mechanical modes at resonance. An accelerometer (Dytran 3100D24T) was attached to different positions around both cryomodules to measure the mechanical vibrations with Agilent 35670A under different conditions. The results are shown in Fig. 3.

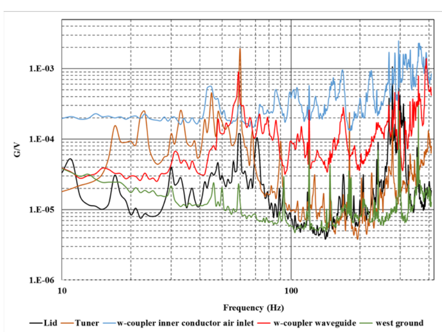

(a)

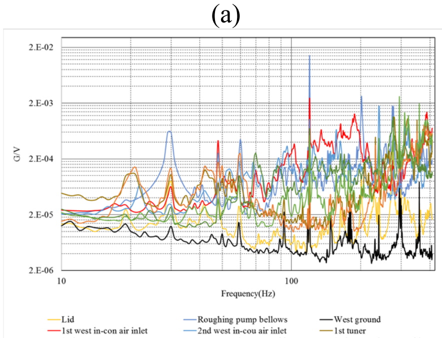

(b)

Figure 3: ICM and ACM1 vibration signals under operational condition: (a) ICM; (b)ACM1

The water pumps for Klystrons cooling, the roughing vacuum pumping bellows and the couplers air cooling flow have been identified as external vibration sources. Most of the noise peaks in Fig. 3 can be found associated with an external source except 40 Hz signal in ICM and 35 Hz signal in both ACM1 cavities. Cryogenic test result reveals the ICM 40 Hz noise is related with JT valve status as shown in Fig. 4. The 40 Hz noise is also found in ACM1 1st cavity with much less amplitude.

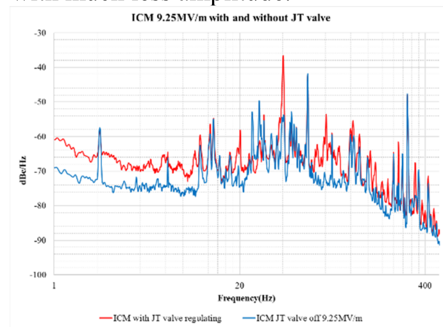

Figure 4: ICM 40 Hz noise and JT valve status. After turning off JT valve the 40 Hz noise peak value decreased about -17 dB.

The 35 Hz is a mechanical mode of cavity as shown in Fig. 5. The external vibration source has not been identified. But it shows correlation with couplers cooling air flow rate and the cooling fans status which was attached on the coupler warm section of the outer conductor.

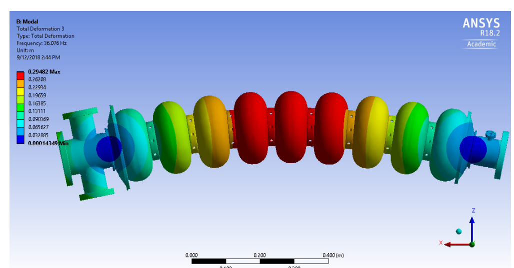

Figure 5: the simulation of 35Hz mode of cavity.

REDUCE EXTERNAL VIBRATION

To improve the beam energy stability, some vibration damping improvements are implemented on both ICM and ACM1 based on the former test results. ACM1 was switched back to vector-sum mode for beam delivery and the vibration damping improvement was implemented step by step with the results shown in Fig. 6.

The ACM1 waveguide damping is temporary proof-of - principle made by wood and rubber inserted between the waveguides and the upper stainless-steel floor near the ACM1. A permanent and optimized damping will be implemented on both ICM and ACM1 waveguide systems in the future.

The ICM vacuum roughing bellows are now fixed and coupler cooling fans are turned off. The most of noise peaks have been reduced as shown in Fig. 7. The coupler cooling air flow optimization and the waveguide vibration absorber installation will be done soon.

DISTURBANCE CAUSED BY LN SYSTEM

The cryomodules use LN_2 for thermal shielding and coupler cooling. The LN_2 supply valve is regulated by the

ISBN: 978-3-95450-194-6 doi:10.18429/JACoW-LINAC2018-TUPO020

cryomodule LN_2 exhaust temperature. The ACM1 RF power shows a correlated fluctuation with the LN_2 supply valve status as shown in Fig. 8.

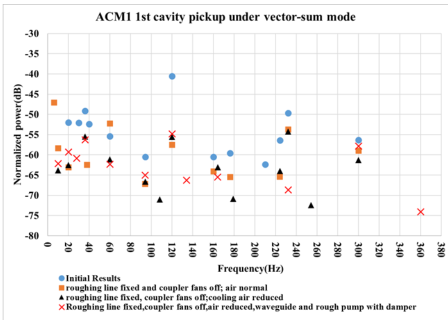

Figure 6: Noise spectra from the phase signal as a function of ACM1 vibration damping. After fixing the roughing bellows and turn off cooling fans most noise peaks are reduced especially the 120 Hz peak; After the cooling air flow is reduced, the noise peaks continue to be reduced with only 3 noise peaks higher than -60 dB; Further damping of the waveguide and the addition of a roughing pump damping pad, the 232 Hz noise peak reduced about -10 dB.

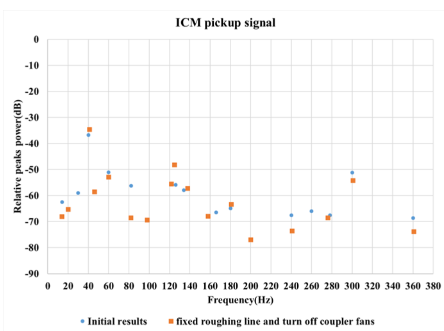

Figure 7: ICM vibration damping.

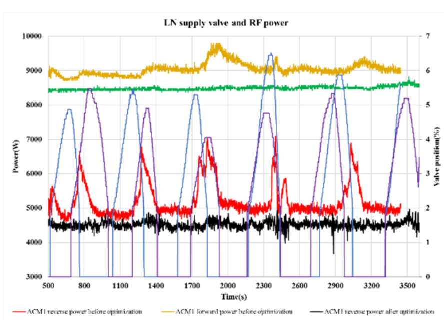

Figure 8: The RF power fluctuation with LN_2 supply valve. The initial regulated temperature was 130K and the reverse power showed 2 kW fluctuation (forward power in yellow and reverse power in red). Then the ACM1 LN_2 regulated temperature decreased to 120 K and the LLRF parameters were optimized, the RF power fluctuation has been reduced (forward power in green and reverse power in black).

After the improvements in Fig. 6, Fig. 7 and Fig. 8 had been implemented, the electron beam was delivered to the final beam dump with 22 MeV (8+7+7) final energy, and the beam energy stability was measured by the BPM which is shown in Fig. 9. The 1mm beam fluctuating translates into about 0.12% of energy fluctuation.

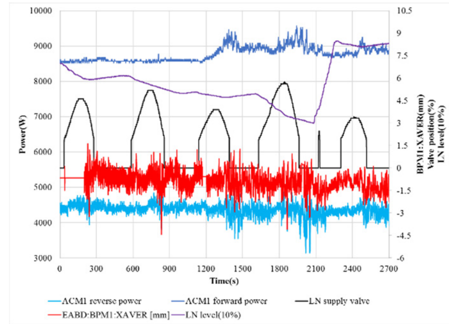

Figure 9: The beam test results with LN_2 supply valve regulated at 120 K. There was still some fluctuation on RF power (forward power in blue and reverse power in green) which became more significant after few LN_2 supply valve opening period (LN_2 level in violet and LN_2 supply valve position in black). The beam energy (red line) had disturbance which correlated with LN valve status.

Then the LN_2 supply valve was switched to constant open mode as shown in Fig. 10.

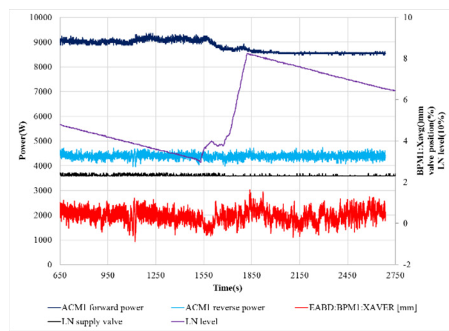

Figure 10: The beam test results with LN_2 supply valve constant open. The fluctuation on beam energy and RF power caused by LN_2 valve has been reduced (in red) and the overall beam energy stability is about ±0.1%. As the LN_2 supply valve (in black) is under constant open mode, the LN_2 tank refilling process (LN_2 level in violet) will affect beam energy (in red) and RF power (forward power in blue and reverse power in green). More optimization need to do on LN_2 system.

DISCUSSION

The stability of ICM and ACM1 cryomodule has been improved and the final beam energy stability is about ±0.1%. In the next step the optimized waveguide damping, coupler cooling air flow rate, water system vibration damping and LN_2 system upgrade will be done. The JT valve mechanical installation and supporter need to be investigated to eliminate the 40 Hz noise. The pickup signals phase monitoring regarding to the reference signal will be set up on EPICS. The effect of the LFD driving ponderomotive instabilities needs further investigation with the threshold presently at a vector sum of 18 MeV.

ISBN: 978-3-95450-194-6 doi:10.18429/JACoW-LINAC2018-TUPO020

ACKNOWLEDGEMENT

ARIEL is funded by the Canada Foundation for Innovation, the Provinces AB, BC, MA, ON, QC, and TRIUMF. TRIUMF receives funding via a contribution agreement with the National Research Council of Canada. The authors would like to thank Tom Powers from JLAB for his inspiring discussion.

REFERENCES

[1] S.R. Koscielniak, *et al.,* “e-Linac photo-fission driver for the Rare Isotope Program at TRIUMF”, in Presented at *PAC’11*, New York, USA, April 2011.

[2] R.E. Laxdal, *et al.*, “The Injector Cryomodule for e-Linac at TRIUMF”, in *Proc. AIP Conf*, vol. 1434, p. 969, 2012. doi.org/10.1063/1.4707014

[3] M. Marchetto *et al.*, “Commissioning and operation of the ARIEL electron LINAC at TRIUMF”, in *Proc. IPAC’15*, Richmond, VA, USA, paper WEYC3, pp. 2444–2449.

[4] Yanyun Ma *et al.*, “First RF test results of two-cavities accelerating cryomodule for ARIEL e-LINAC at TRIUMF”, in *Proc. IPAC’18*, Vancouver, BC, Canada, pp. 4512-4515.. doi:10.18429/JACoW-IPAC2018- THPMK090

[5] Ken Fong *et al.*, “Tuners alignment on two 9-cell cavities with single amplifier under self-excited loop”, in *Proc. IPAC’18*, Vancouver, BC, Canada, pp.4527-4529 doi:10.18429/JACoW-IPAC2018- THPMK096